



## 37        **1. Introduction**

38    Reactive carbonyl species (RCS) are a class of breakdown products arising from the  
39    oxidation of sugars and lipids which can be formed either exogenously, for instance during  
40    food processing or cooking, and endogenously, via different pathophysiological conditions.  
41    RCS are chemically quite heterogeneous, belonging to different classes, including di-  
42    aldehydes, cheto-aldehydes and alpha,beta-unsaturated aldehydes. RCS have the common  
43    property of covalently reacting with nucleophilic substrates such as proteins. Covalent  
44    adducts originating from lipids are named ALEs (advanced lipoxidation end-products),  
45    whereas RCS originating from sugars are known as AGEs (advanced glycoxidation end-  
46    products). Since the 1980s, RCS and their corresponding reaction products have been  
47    widely used as markers of oxidative stress and several analytical methods for their  
48    measurements have been developed and widely applied. More recently, due to growing  
49    body of evidence reporting the involvement of AGEs and ALEs in the onset and propagation  
50    of some human diseases, RCS have been considered not only as biomarkers but also as  
51    potential drug targets. Among the damaging RCS, HNE is one of the most studied since its  
52    discovery by Hermann Esterbauer in 1964, due to its abundance, reactivity, and biological  
53    effects (Poli, Schaur, Siems, & Leonarduzzi, 2008). The strict link between elevated HNE  
54    tissue/blood levels and some human diseases suggests a potential link in the  
55    pathophysiology. Several studies based on cell signaling and protein covalent modification  
56    have since reported the molecular mechanisms involved in the cytotoxic effect of HNE.  
57    Different molecular approaches for reducing the overproduction of HNE and in general of  
58    RCS have been reported and summarized in some recent reviews (Giancarlo Aldini, Dalle-  
59    Donne, Facino, Milzani, & Carini, 2007). Among the proposed approaches, the most  
60    promising is based on small nucleophilic molecules (RCS sequestering agents) which  
61    covalently react with RCS, forming unreactive adducts which are then metabolized and  
62    excreted. Several RCS sequestering agents have been proposed such as aminoguanidine,  
63    pyridoxamine, hydralazine and carnosine and their protective effects in animal models, as  
64    confirmed by several independent labs, further underline the promising therapeutic efficacy  
65    of targeting HNE (Colzani et al., 2016) . Carnosine has recently been reported as the most  
66    efficient and selective sequestering agent of HNE and its promising activity has been  
67    demonstrated in animal models and most recently in obese subjects (Giancarlo Aldini et al.,  
68    2011). However, the application of carnosine as HNE sequestering agent in humans is  
69    limited because of its poor bioavailability, due to the presence of serum carnosinases, which  
70    catalyze the hydrolytic cleavage of the dipeptide. Nowadays there is great interest in the

71 discovery of novel HNE sequestering agents such as carnosine derivatives resistant to  
72 carnosinases.

73 Among others, an interesting discovery approach to identify novel HNE sequestering agents  
74 is that based on searching for bioactive compounds in plant extracts. Plants are also subject  
75 to RCS stress, in particular mediated by alpha,beta-unsaturated aldehydes, HNE being the  
76 most abundant and toxic carbonyl compound formed in stress conditions. Because plants  
77 are subject to RCS and protein carbonylation damage (Biswas & Mano, 2016), they have  
78 developed efficient enzymatic and non-enzymatic detoxification pathways. Hence, besides  
79 detoxifying enzymes, it is reasonable to consider the presence of secondary metabolites  
80 acting as RCS sequestering agents. Such a hypothesis has been partially confirmed by  
81 previous studies which have reported that EGCG and other polyphenols are effective as  
82 sequestering agents of HNE (Beretta, Furlanetto, Regazzoni, Zarrella, & Facino, 2008) and  
83 of other RCS, including acrolein and methylglyoxal. These results prompted scientists to  
84 screen the sequestering activity of different plant metabolites and, in particular, the  
85 polyphenol class. As an example, Zhu et al. compared 21 natural polyphenols with diverse  
86 structural characteristics for their ACR-/HNE-trapping capacities under simulated  
87 physiological conditions (Zhu et al., 2009).

88 To the best of our knowledge, the search for a potential RCS natural sequestering agent  
89 has been carried out by using isolated molecules or highly purified extracts and not by  
90 applying off-target methods involving crude extracts. One reason is the lack of analytical  
91 methods able to test the sequestering activity of complex matrices and the inherent  
92 difficulties associated with fishing out compounds that are bioactive. As an example, one of  
93 the most used methods to evaluate HNE sequestering efficacy is based on a HPLC-UV  
94 method for measuring the residual amount of HNE. Such an approach is clearly suitable for  
95 testing single molecules and not mixtures, which would interfere with HNE analysis.

96 We have recently reported an *in vitro* high-resolution MS method to test the ability of  
97 compounds, mixtures and extracts to trap RCS by measuring their efficacy in inhibiting  
98 ubiquitin carbonylation induced by reactive carbonyl species including HNE (Colzani et al.,  
99 2014). Such a method was found suitable to evaluate the overall quenching activity of  
100 extracts, however it does not permit the identification of the active components.

101 In the present paper we report an LC-ESI-MS method based on an isotopic labelling  
102 procedure which permits the identification of the HNE sequestering agents contained in a  
103 crude mixture. Together with the ubiquitin method, it was then applied to search for HNE  
104 sequestering agents contained in extracts prepared from different varieties of rice.

105

## 106 **2. Materials and Methods**

### 107 2.1. Chemicals

108 Formic acid (HCOOH), sodium dihydrogen phosphate ( $\text{NaH}_2\text{PO}_4 \cdot \text{H}_2\text{O}$ ), sodium hydrogen  
109 phosphate ( $\text{Na}_2\text{HPO}_4 \cdot 2\text{H}_2\text{O}$ ), phenylalanine, gamma-aminobutyric acid, histidine, triclin-5-  
110 o-glucoside, lyophilized ubiquitin from bovine erythrocytes (BioUltra,  $\geq 98\%$ ) and LC–MS  
111 grade solvents were purchased from Sigma–Aldrich (Milan, Italy). Peonidin-3-O-glucoside,  
112 malvidin, peonidin and pelargonidin were from Extrasynthese (Genay, France). Carnosine  
113 (beta-alanyl-L-histidine) was a generous gift from Flamma S.p.A (Chignolo d'Isola,  
114 Bergamo, Italy). LC-grade  $\text{H}_2\text{O}$  (18 M $\Omega$  cm) was prepared with a Milli-Q  $\text{H}_2\text{O}$  purification  
115 system (Millipore, Bedford, MA, USA). All other reagents were of analytical grade. 4-  
116 hydroxy-2-nonenal diethylacetal (HNE-DEA) and  $^2\text{H}_5$ -4-hydroxy-2-nonenal diethylacetal  
117 ( $^2\text{H}_5$ -HNE-DEA) were synthesized according to the literature (Rees, van Kuijk, Siakotos, &  
118 Mundy, 1995) and stored at  $-20^\circ\text{C}$ . For each experiment, fresh 4-hydroxy-2-nonenal (HNE)  
119 was prepared starting from stored HNE-DEA, which was evaporated under nitrogen stream  
120 and hydrolyzed with 1 mM HCl, pH 3 for 1 h at room temperature to obtain HNE. The  
121 concentration of HNE was estimated by measuring the absorbance at  $\lambda = 224$  nm (molar  
122 extinction coefficient =  $13,750 \text{ M}^{-1} \times \text{cm}^{-1}$ ).

123

### 124 2.2. Plant material

125 Black rice with giant embryo and white rice were provided by the National Institute of Crop  
126 Science, Rural Development Administration, Republic of Korea. A detailed method for the  
127 development and culture of black rice with giant embryo has been previously reported (Kim  
128 et al., 2013).

129 Rice extract preparation: the seeds were manually dehulled with a wooden rice dehuller and  
130 ground to a powder by using a mortar and pestle. The milled rice powders were stored at  
131  $-80^\circ\text{C}$  until further use. Water extract of black rice with giant embryo was provided by  
132 National Institute of Crop Science, Rural Development Administration, Republic of Korea.  
133 200 g of BRGE was extracted with 200 mL of water for 5 days at room temperature, and the  
134 extracts were filtered and evaporated under vacuum, followed by drying. The yield of  
135 extraction was 4.32%.

136 Rice extract filtration: for the ubiquitin assay as well as for the isotopic labelling procedure,  
137 rice powder extracts were then dissolved in water and ultrafiltered by using a 3 kDa  
138 ultrafilters so to remove proteins and high M.W. components. The yield of the low molecular

139 fraction after 3 kDa ultrafiltration was  $\approx$  10% of the starting sample for all the rice varieties  
140 tested.

141

### 142 2.3. Ubiquitin carbonylation assay

143 The effect of rice extracts on HNE-induced protein carbonylation was tested by using the  
144 ubiquitin assay as previously reported. Briefly, ubiquitin (10  $\mu$ M final concentration) was  
145 chosen as the protein target of HNE induced protein adduction. Ubiquitin was incubated for  
146 24 h at 37 °C in 10 mM phosphate buffer in the presence of 500  $\mu$ M HNE together with rice  
147 extracts of increasing concentrations (10, 25 and 50 mg/mL). To remove high molecular  
148 components, which could interfere with the assay, the rice extracts were filtered by using  
149 Amicon YM3 filters (Millipore, Milan, Italy) and the filtered fractions were then used for the  
150 assay. After an incubation time of 24 h, the reactions were stopped by centrifugation using  
151 Amicon YM3 filters and the extent of ubiquitin carbonylation was determined by MS intact  
152 protein analysis using the microflow automated loop injection procedure as already  
153 described (Colzani et al., 2014).

154

### 155 2.4. Identifying the HNE sequestering agents by an isotopic labelling procedure

156 After filtration by using Amicon YM3 filters, the black rice giant embryo extract (BRGE) was  
157 dissolved in PBS at a final concentration of 50 mg/mL and was then incubated for 24 hours  
158 in presence of HNE or deuterium labelled HNE ( $^2\text{H}_5$ -HNE). Control samples were incubated  
159 neither with HNE nor with deuterium labelled HNE. After 24 hours the samples were  
160 analyzed individually by LC-MS together with a sample prepared by mixing in a 1:1 v/v ratio  
161 the samples incubated with HNE and  $^2\text{H}_5$ -HNE. LC-HRMS were run in positive and negative  
162 ion mode.

163

#### 164 2.4.1. *Chromatographic conditions*

165 Chromatographic separation was performed on a reversed-phase Agilent Zorbax SB-C18  
166 column (150 x 2.1 mm, i.d. 3.5  $\mu$ m, CPS analitica, Milan, Italy), protected by an Agilent  
167 Zorbax guard column, by an UltiMate 3000 system (Dionex) equipped with an autosampler  
168 kept at 4°C working at a constant flow rate (200  $\mu$ L/min). 10  $\mu$ L of sample was injected into  
169 the column and the analytes were eluted with a 45 min multistep gradient of phase A H<sub>2</sub>O-  
170 HCOOH (100:0.1, v/v) and phase B CH<sub>3</sub>CN-HCOOH (100:0.1, v/v): 0-5 min, isocratic of 1%  
171 B; 5-15 min, from 1% B to 25% B; 15-30 min, from 25% B to 65% B; 30-32 min, from 65%

172 B to 80% B; 32-36 min, isocratic of 80% B; 36-36.1 min, from 80% B to 1 % B, and then  
173 36.1-45 min of isocratic 1% B.

#### 174 2.4.2. MS conditions

175 The acquisitions were performed on a LTQ-Orbitrap XL mass spectrometer (Thermo Fisher  
176 Scientific, San Jose, USA) using an ESI source, acquiring in positive and in negative ion  
177 mode. A real-time mass calibration was obtained by using a list of 20 background ions  
178 (Keller, Sui, Young, & Whittal, 2008). The source parameters used for the positive mode  
179 are: spray voltage 3 kV, capillary temperature 275 °C, capillary voltage 49 V, sheath gas  
180 flow 15 units, auxiliary gas flow 5 units, tube lens offset 130 V; for the negative ion mode:  
181 spray voltage 3.5 kV, capillary temperature 275 °C, capillary voltage -17 V, sheath gas flow  
182 15 units, auxiliary gas flow 5 units, tube lens offset -100 V. Full MS spectra were acquired  
183 in profile mode by the FT analyzer in a scan range of 100-1000  $m/z$ , using AGC scan target  
184  $5 \times 10^5$  and resolution 100000 FWHM at 400  $m/z$ . Tandem mass spectra were acquired by  
185 the linear ion trap (LTQ) that was set up to fragment the 3 most intense ions exceeding  $1 \times$   
186  $10^3$  counts. Mass acquisition settings were: centroid mode, AGC scan target  $1 \times 10^4$ ,  
187 precursor ion isolation width of 2.5  $m/z$ , and collision energy (CID) of 30 eV. Dynamic  
188 exclusion was enabled to reduce redundant spectra acquisition: 2 repeat counts, 20 sec  
189 repeat duration, 30 sec of exclusion duration. Instrument control and spectra analysis were  
190 provided by the software Xcalibur 2.0.7 and Chromeleon Xpress 6.80.

191

#### 192 2.5. HPLC-UV HNE sequestering assay

193 The compounds identified as putative HNE binders with the method described in section 2.4  
194 were purchased as pure standards and tested individually for their HNE sequestering ability.  
195 The assay was a three-hour time course experiment at pH 7.4 and 37 °C, in the presence  
196 of 50  $\mu$ M HNE and 1 mM of the tested compound. The residual HNE was measured hourly  
197 within a three-hour reaction time by using the HPLC-UV assay described by Vistoli et al.  
198 (Vistoli et al., 2009) with some minor modifications. Briefly, HNE concentration was  
199 determined by a Surveyor HPLC platform (ThermoScientific, Milan, Italy) setting the UV  
200 detector at 224 nm. HNE elution was performed in 6 minutes by reverse phase  
201 chromatography at 37 °C and flow rate of 0.3 mL/min. A Kinetex column (75 mm x 2.1 mm  
202 i.d., 2.6  $\mu$ m particle size, 100 Å porosity, Phenomenex, Castel Maggiore, Italy) was used as  
203 stationary phase, while mobile phase consisted of H<sub>2</sub>O-CH<sub>3</sub>CN-HCOOH, 80:20:0.1 (v/v/v).  
204 The amount of reacted HNE was calculated by the following formula:

205

206  
207  
208  
209  
210  
211  
212  
213  
214  
215  
216  
217  
218  
219  
220  
221  
222  
223  
224  
225  
226  
227  
228  
229  
230  
231  
232  
233  
234  
235  
236  
237  
238

$$reacted\ HNE\ (\%) = \frac{[HNE]_{t0} - [HNE]_{t3}}{[HNE]_{t0}} \times 100$$

[HNE]<sub>t0</sub> being the concentration of HNE at the beginning of the incubation and [HNE]<sub>t3</sub> being the concentration of HNE at the end of the incubation. Carnosine, which is a HNE sequestering agent not containing a thiol moiety, was used as positive control to assess the assay reproducibility. To demonstrate that HNE consumption over time is not caused by auto-oxidation, an incubation in pure phosphate buffer was performed as negative control. The activity of each compound was also given as Carnosine Units (i.e. the ratio between the % of HNE reacted with the compound at a given time and the % of HNE reacted with carnosine in the same span of time).

## 2.6. Computational studies

For simplicity, attention was focused on two anthocyanidins chosen as representative of active (pelargonidin) and inactive (malvidin) compounds. Given the tested physiological pH, the compounds were simulated in their quinodal neutral form by considering three major tautomers. In order to investigate their stereo-electronic properties, these structures were minimized at their ground-state and at gas phase by density functional theory (DFT) using the Becke three-parameter hybrid function with LYP correlation (DFT/B3LYP) and with the 6-31G basis set as implemented by the GAMESS software (Schmidt et al., 1993).

## 3. Results and discussion

### 3.1. Overview of the approach

RCS are well-known pathogenetic factors of various oxidative based diseases and recently molecular approaches based on their detoxification properties, and have been found effective in preventing the onset and progression of some diseases in different animal models. Among the different strategies aimed at detoxifying RCS, those based on small nucleophilic compounds capable of trapping and detoxifying RCS are of interest. Several synthetic and natural RCS sequestering agents have so far been reported to be effective in several animal models, but for many of these compounds, clinical application is limited due to their ill-defined activity, lack of selectivity and of suitable bioavailability. Hence, a discovery approach aimed at identifying novel RCS sequestering agents is necessary to overcome this gap. In the present paper, we report a discovery approach aimed at identifying

239 RCS sequestering agents in crude mixtures such as natural extracts. Natural sources and,  
240 in particular, plant extracts, represent an attractive source of RCS sequestering agents due  
241 to the fact that plants are also subject to RCS stress, in particular mediated by  $\alpha,\beta$ -  
242 unsaturated aldehydes, and that they have developed efficient enzymatic and non-  
243 enzymatic detoxification pathways. Many non-enzymatic pathways and in particular those  
244 based on small nucleophilic agents are still unexplored and they would represent an  
245 interesting potential source of novel bioactive compounds.

246 Searching for RCS sequestering agents in a crude mixture is quite a challenging process  
247 because they are usually present as minor components in respect to the complex matrix,  
248 making their identification and characterization analytically challenging. Moreover, a robust  
249 method capable of measuring the overall RCS sequestering activity is needed in order to  
250 select and identify the most effective plant extracts.

251

252 Here we report a new method to overcome these challenges that is based on the following  
253 steps: i) the RCS sequestering activity of the tested extracts is first characterized by using  
254 the ubiquitin assay as previously reported; ii) the most active extracts are then selected in  
255 order to identify sequestering agents by using an innovative isotopic labelling procedure, iii)  
256 the RCS sequestering activities of the identified compounds are then validated by using  
257 standard compounds and using an HPLC-UV method.

258 The method proposed has been applied by using HNE as target aldehyde and eight rice  
259 extracts as potential sources of RCS sequestering agents. HNE is an  $\alpha,\beta$ -unsaturated  
260 aldehyde generated endogenously and exogenously (it is present in food) by the radical-  
261 mediated peroxidation of  $\omega$ -6 polyunsaturated fatty acids. Since its identification, 4-hydroxy-  
262 nonenal (HNE), an autoxidation product of unsaturated fats and oils (at first erroneously  
263 described as 4-hydroxy-octenal) (Schaur, Siems, Bresgen, & Eckl, 2015), has attracted  
264 great scientific interest, as demonstrated by the publication of more than 4200 papers since  
265 1980. Compared to other 4-hydroxyalkenals, HNE is the most extensively studied and  
266 reviewed as it was the first one discovered (Schaur et al., 2015), it represents the main 4-  
267 hydroxyalkenal formed during the autoxidation of unsaturated fatty acids (Catalá, 2009), it  
268 is highly reactive (Poli & Schaur, 2000) and numerous biological effects have been  
269 demonstrated (Catalá, 2009), leading HNE being considered as a promising drug target.

270 Rice (*Oryza sativa*) is one of the five different cereal grains, which are the most commonly  
271 consumed throughout the world and are functionally reported to have antioxidant activity.  
272 Bioactive components of rice, have demonstrated antioxidant and anti-inflammatory



273 activities in cells and animals (Lee, Han, Song, & Yeum, 2015; Masisi, Beta, & Moghadasian,  
274 2016).

275 However, although the direct and indirect antioxidant activity of rice has been demonstrated  
276 in different *in vitro* and also *in vivo* models, no data to our knowledge have so far been  
277 reported regarding the efficacy of rice towards protein carbonylation and, in particular, its  
278 ability to sequester RCS. We then decided to apply the proposed method to test the RCS  
279 sequestering capability of rice and so we evaluated the water extracts of white, brown and  
280 black rice.

281

### 282 3.2. HNE sequestering activity of rice extracts

283 The overall HNE sequestering activity of eight rice extracts was studied using the ubiquitin  
284 assay as previously reported. The method consists of incubating ubiquitin as protein target  
285 with HNE at a specific molar ratio and incubation time, thus inducing ubiquitin covalent  
286 modification of almost 50%. The protein carbonylation was monitored by measuring the ratio  
287 of the areas of two peaks: one at  $m/z$  779.61239 relative to the 11-charged peak (named  
288 z11) of native ubiquitin and the second at  $m/z$  793.80415 corresponding to the 11-charged  
289 peak of ubiquitin covalently modified by HNE. **Figure 1** shows the MS spectra of ubiquitin  
290 incubated in the absence and in the presence of HNE. When ubiquitin incubated with HNE  
291 was spiked with rice extracts, a dose-dependent reduction of the peak area relative at  $m/z$   
292 793.80415 was observed. The  $IC_{50}$  value, which is the rice extract concentration able to  
293 decrease by 50% the level of protein carbonylation, was determined. **Table 1** summarizes  
294 the  $IC_{50}$  of the tested rice extracts. White rice extract was found less effective in respect to  
295 colored rice and of these, black rice with giant embryo was the most effective and for this  
296 reason it was selected for the next step aimed at identifying the compounds responsible for  
297 the sequestering effect of the extract.

298

299

### 300 3.3. Set-up of an isotopic labelling procedure for the identification of HNE- 301 sequestering agents

302 An off-target approach based on isotopic signature was then set-up to identify HNE  
303 adducted compounds when present in complex matrices such as plant extracts. As  
304 summarized in **Figure 2**, the method consists of the following steps: i) the plant extract is  
305 spiked with HNE (156.11502 Da) and  $^2H_5$ -HNE (161.07590 Da) mixed at the same molar  
306 ratio. Compounds which are reactive towards HNE, react with both the isotopes at the same

307 rate forming reaction products which have a specific isotopic pattern. A pair of peaks with a  
308 similar intensity spaced by the delta mass corresponding to the incremental mass of  $^2\text{H}_5$ -  
309 HNE with respect to HNE (5.03088 Da  $\pm$  10 ppm) is generated. The second step consists of  
310 extracting the  $m/z$  values relative to the ions of the HNE adducts. This is automatically  
311 carried out by Compound Discoverer<sup>TM</sup> on the basis of the specific isotopic pattern  
312 characterized by the two peaks with the same intensity and with a delta mass corresponding  
313 to five deuterium atoms. **Figure 3** shows in more detail the specific workflow generated to  
314 extract the peak lists from the mass spectra. By setting the "Pattern Tracer" node with a  
315 delta mass of 5.03088 Da, a chromatogram of the peak pairs characterized by the set delta  
316 mass was obtained. Elution times of the most abundant peaks were then extracted and the  
317  $m/z$  values of each peak pair were then obtained by the TIC chromatogram. HNE adducts  
318 were then confirmed by manually inspecting the characteristic relative abundance and mass  
319 shift of the isotopic pattern.

320 Further confirmation of the identity of the HNE adducts was given by the *Unknown Detector*  
321 *node* which checks for the absence of the detected peaks as above reported in non-spiked  
322 samples.

323 As a final adduct confirmation, the MS/MS spectra of each ion of the isotopic pattern (non-  
324 deuterated and deuterated ions) were checked in order to verify the overlap between the  
325 spectra, thus confirming the same structures and avoiding false positives. The M.W. of the  
326 bioactive compounds were then calculated by subtracting the M.W. of the HNE molecule  
327 ( $\approx$ 156 Da) from the masses of the identified compounds, and assuming that the detected  
328 ions are attributed to the Michael adduct between HNE and the bioactive molecule (as  
329 reported for a series of bioactive molecules able to quench HNE (G Aldini, Facino, Beretta,  
330 & Carini, 2005)).

331 The method was firstly validated by using GSH and carnosine as known sequestering  
332 agents. **Figure 4** shows the Full MS and MS/MS spectra of the GSH spiked with HNE and  
333  $^2\text{H}_5$ -HNE mixed at the same molar ratio. The GSH-HNE and GSH- $^2\text{H}_5$ -HNE adducts are  
334 present as single charged ions at 464.20629  $m/z$  and 469.23712  $m/z$ . They are also present  
335 as  $[\text{M}+\text{H}-\text{H}_2\text{O}]^+$  ions as shown in **Figure 4A**. The fragmentation patterns are characterized  
336 by the  $\text{H}_2\text{O}$  loss and the HNE and  $^2\text{H}_5$ -HNE neutral loss (**Figure 4B** and **C**), giving the ion at  
337 308.1  $m/z$  that is the GSH moiety.

338

339 3.4. Identification of sequestering components in black rice with giant embryo

340 **Figure 5** shows the pattern trace of BRGE incubated in the presence of HNE and  $^2\text{H}_5$ -HNE  
341 mixed at the same molar ratio. Eleven peaks over the threshold intensity were easily  
342 identified and their HNE adducted nature was confirmed by manual inspection taking into  
343 account the mass shift between the ion pairs, their relative abundances and the overlapping  
344 MS/MS fragmentation pattern. The M.W. of the sequestering agents were then determined  
345 by subtracting the adduct M.W. from that of HNE. The identity of the parent compounds was  
346 then assigned by matching the experimental accurate masses and MS/MS fragment ions  
347 with those contained in a database of compounds compiled by including the chemicals  
348 contained in rice (Abdel-Aal, Young, & Rabalski, 2006; Goufo & Trindade, 2014; Pereira-  
349 Caro, Cros, Yokota, & Crozier, 2013; Suttiarporn et al., 2015). The database contained 112  
350 entries (32 anthocyanins, 14 phenolic acids, 22 between flavones and flavonols, 9  
351 tocopherols, 20 Ferulates ( $\gamma$ -orizanol), 4 carotenoids, 7 sterols and 4 triterpenoids. A list of  
352 nine compounds with a M.W. lower than 350 Da was then obtained and listed in **Table 2**.  
353 Five out of 9 compounds were flavonoids, four of them belonging to the anthocyanidins  
354 class, three compounds were aminoacids, two of them proteogenic, while one a peptide.

355

### 356 3.5. HNE sequestering activity

357 The commercially available compounds identified as described in section 3.4 were then  
358 tested as HNE sequestering agent by using an HPLC-UV test. The test is based on  
359 measuring free-HNE after incubating the tested compound with HNE. **Table 3** reports the  
360 percentage of HNE sequestered by the active compounds identified in BRGE extract.  
361 Results are reported either as % of HNE consumption at 1 and 3 hours and as carnosine  
362 units at 1 and 3 hours, setting as 1 the value of carnosine activity for both the time points.  
363 Histidine, phenylalanine and aminobutyric acid were the aminoacids identified as having  
364 HNE sequestering activity. The reactivity for histidine is due to the imidazole ring as has  
365 already been reported, together with the full elucidation of the reaction adduct by NMR. The  
366 activity of histidine is increased when bonded to specific aminoacids such as beta-alanine,  
367 as in the case of carnosine, or analogues, which are histidine peptides found in mammals.  
368 However, no histidine peptides were detected as HNE adducts in the rice extract. The HNE  
369 sequestering activity of GABA and phenylalanine, which is more likely due to their primary  
370 amino group, is very weak and much lower in respect to that of carnosine (the HNE  
371 sequestering activity was under the detection limit as determined by using the HPLC-UV  
372 assay). However, even if these two compounds are characterized by a very low potency as  
373 HNE sequestering agents in comparison to that of carnosine, they act as HNE sequestering

374 agents in the crude mixture. This apparent contradiction could be explained by considering  
375 that they are probably contained in high concentrations in the extract or could be explained  
376 by the specific milieu which catalyses their reactions. In other words, it should be considered  
377 that the overall sequestering efficacy of compounds in plant extracts is not only due to their  
378 intrinsic nucleophilic reactivity but also to their relative concentration as well as to the matrix  
379 which could affect the intrinsic activity itself.

380 A set of polyphenols were then identified as HNE sequestering agents, four anthocyanidins  
381 and one flavone (tricin). All of the identified compounds were found to be less effective than  
382 carnosine but characterized in the HPLC-UV assay by a well detectable activity. Among  
383 these polyphenols, pelargonidin was the most potent, followed by triclin, peonidin and  
384 malvidin. The activity of anthocyanidins as HNE sequestering agents which are  
385 characteristic components of black rice can also explain the higher overall activity of black  
386 rice in respect to white rice and to the other rice varieties.

387

### 388 3.6. Anthocyanidins as HNE sequestering agents: molecular modelling studies

389 As evidenced by several studies investigating various adducts on anthocyanidins, the C8  
390 atom is the most prone centre for the electrophilic attack. As exemplified by the  
391 pelargonidine tautomers in **Figure 6**, DFT calculations showed that the electron density at  
392 C8 vastly differs in the three simulated major tautomers. These differences, which are  
393 similarly detected in both considered compounds, revealed that the N7 tautomers are the  
394 most electron rich one at C8 due to the effect of the vicinal deprotonation in 7, while the N4'  
395 tautomers are the least electron rich one at C8 due to the electron-drawing effect exerted  
396 by the C4'deprotonation. While showing comparable stereo-electronic features, **Table 4**  
397 reveals that the tautomers of pelargonidin and malvidin greatly differ in their relative stability.  
398 In detail, **Table 4** shows that the N7 tautomer is the most stable for pelargonidin, while the  
399 N5 tautomer is the preferred one for malvidin and the C4' tautomer is the least stable form  
400 for both anthocyanidins. **Table 4** also evidences that the nucleophilicity differences, despite  
401 being very limited, parallel the tautomer stability, the pelargonidin N7 tautomer being the  
402 most nucleophilic species.

403 These results are in agreement with the previous similar calculations performed by Estevez  
404 et al. (Estévez & Mosquera, 2009) and suggest that the observed differences in the  
405 quenching activity between pelargonidin and malvidin are ascribable to different relative  
406 abundance of the reactive N7 tautomer, while the differences in the stereo-electronic  
407 properties, while confirming the highest nucleophilicity of the pelargonidin N7 tautomer,

408 appear to be too limited to explain alone the different reactivity towards HNE. Taken  
409 together, these results confirm that the relative tautomer stability is markedly influenced by  
410 the substituents on the B ring and suggest that the stability of the reactive N7 tautomer is  
411 lowered by electron-donating groups on the B ring, a finding which may explain the  
412 intermediate reactivity of peonidin.

413

#### 414 **4. Conclusion**

415 In conclusion, we report a novel approach, which permits the screening of plant extracts and  
416 in general complex matrices for their overall activity as HNE sequestering agents and the  
417 identification of small molecules responsible for the sequestering effects. This approach  
418 could be applied to screen a variety of plant extracts with the final aim of identifying novel  
419 and potent HNE sequestering agents. These methods can also be easily adapted to other  
420 cytotoxic RCS compounds such as MDA, glyoxal and methylglyoxal for which potent  
421 sequestering agents are yet to be found.

422

423 By using this assay, we also found that rice, and in particular black rice is a valuable source  
424 of detoxifying agents of HNE which is known to be formed during food digestion and has a  
425 role in the promotion of colon cancer (Bastide et al., 2015). HNE derived from food is  
426 estimated to be  $16 \mu\text{g day}^{-1}$  as daily exposure in korean food for a 60 Kg korean adult (Surh  
427 & Kwon, 2005). Based on the fact that 29.1 mg, corresponding to 673 mg black rice, inhibits  
428 50% of protein carbonylation induced by  $78.0 \mu\text{g mL}^{-1}$  of HNE we can easily conclude that  
429 the HNE daily exposure of  $16 \mu\text{g day}^{-1}$  should be easily detoxified by a serving portion of 75  
430 gr.

431

#### 432 **5. Acknowledgments**

433

#### 434 **Figure legends**

435 **Figure 1** - 11-charged MS peaks of ubiquitin incubated in the absence and in the presence  
436 of HNE and increasing concentration of two extract: white rice extract (panel on the left) and  
437 BRGE (panel on the right).

438 **Figure 2** – Graphic representation of the method.

439 **Figure 3** – Workflow's nodes used in Compound Discoverer.

440 **Figure 4** – Full MS and MS/MS spectra of GSH spiked with HNE and  $^2\text{H}_5$ -HNE mixed at  
441 the same molar ratio. A) Full MS spectrum showing the ions at  $464.20629 m/z$  and at

442 446.19599  $m/z$ , which represent the  $[M+H]^+$  and the  $[M+H-H_2O]^+$  respectively of GSH-  
443 HNE, and the ions at 469.23712  $m/z$  and at 451.22736  $m/z$ , which are the  $[M+H]^+$  and the  
444  $[M+H-H_2O]^+$  respectively of GSH- $^2H_5$ -HNE. B) MS/MS spectrum of GSH-HNE adduct: the  
445 ion at 446.06  $m/z$  derives from the loss of  $H_2O$  and the ion at 308.12  $m/z$  which is the GSH  
446 moiety deriving from the neutral loss of HNE. C) MS/MS spectrum of GSH- $^2H_5$ -HNE  
447 adduct: the ion at 451.09  $m/z$  derives from the loss of  $H_2O$  and the ion at 308.11  $m/z$  which  
448 is the GSH moiety deriving from the neutral loss of  $^2H_5$ -HNE.

449 **Figure 5** - The “pattern tracer” chromatogram obtained by Compound Discoverer of BRGE  
450 + HNE +  $^2H_5$ -HNE (negative ion mode).

451 **Figure 6** - DFT-based molecular electrostatic potential (MEP) as projected on solvent  
452 accessible surface for the three major pelargonidin tautomers. The brown arrow indicates  
453 the C8 electrophilic attack center in the most nucleophilic tautomer.

454

455

## References

- 456 Abdel-Aal, E. S. M., Young, J. C., & Rabalski, I. (2006). Anthocyanin composition in black,  
457 blue, pink, purple, and red cereal grains. *Journal of Agricultural and Food Chemistry*,  
458 54(13), 4696–4704. <https://doi.org/10.1021/jf0606609>
- 459 Aldini, G., Dalle-Donne, I., Facino, R. M., Milzani, A., & Carini, M. (2007). Intervention  
460 strategies to inhibit protein carbonylation by lipoxidation-derived reactive carbonyls.  
461 *Medicinal Research Reviews*. <https://doi.org/10.1002/med.20073>
- 462 Aldini, G., Facino, R. M., Beretta, G., & Carini, M. (2005). Carnosine and related dipeptides  
463 as quenchers of reactive carbonyl species: from structural studies to therapeutic  
464 perspectives. *Biofactors*, 24(1–4), 77–87. <https://doi.org/10.1002/biof.5520240109>
- 465 Aldini, G., Orioli, M., Rossoni, G., Savi, F., Braidotti, P., Vistoli, G., ... Carini, M. (2011).  
466 The carbonyl scavenger carnosine ameliorates dyslipidaemia and renal function in  
467 Zucker obese rats. *Journal of Cellular and Molecular Medicine*, 15(6), 1339–1354.  
468 <https://doi.org/10.1111/j.1582-4934.2010.01101.x>
- 469 Bastide, N. M., Chenni, F., Audebert, M., Santarelli, R. L., Taché, S., Naud, N., ... Pierre,  
470 F. H. F. (2015). A central role for heme iron in colon carcinogenesis associated with  
471 red meat intake. *Cancer Research*, 75(5), 870–879. [https://doi.org/10.1158/0008-](https://doi.org/10.1158/0008-5472.CAN-14-2554)  
472 5472.CAN-14-2554
- 473 Beretta, G., Furlanetto, S., Regazzoni, L., Zarrella, M., & Facino, R. M. (2008). Quenching  
474 of alpha,beta-unsaturated aldehydes by green tea polyphenols: HPLC-ESI-MS/MS  
475 studies. *Journal of Pharmaceutical and Biomedical Analysis*, 48(3), 606–611.

476 <https://doi.org/10.1016/j.jpba.2008.05.036>

477 Biswas, M. S., & Mano, J. (2016). Reactive carbonyl species activate caspase-3-like  
478 protease to initiate programmed cell death in plants. *Plant and Cell Physiology*, 57(7),  
479 1432–1442. <https://doi.org/10.1093/pcp/pcw053>

480 Catalá, A. (2009). Lipid peroxidation of membrane phospholipids generates hydroxy-  
481 alkenals and oxidized phospholipids active in physiological and/or pathological  
482 conditions. *Chemistry and Physics of Lipids*.  
483 <https://doi.org/10.1016/j.chemphyslip.2008.09.004>

484 Colzani, M., Criscuolo, A., De Maddis, D., Garzon, D., Yeum, K. J., Vistoli, G., ... Aldini, G.  
485 (2014). A novel high resolution MS approach for the screening of 4-hydroxy-trans-2-  
486 nonenal sequestering agents. *Journal of Pharmaceutical and Biomedical Analysis*, 91,  
487 108–118. <https://doi.org/10.1016/j.jpba.2013.12.024>

488 Colzani, M., De Maddis, D., Casali, G., Carini, M., Vistoli, G., & Aldini, G. (2016).  
489 Reactivity, Selectivity, and Reaction Mechanisms of Aminoguanidine, Hydralazine,  
490 Pyridoxamine, and Carnosine as Sequestering Agents of Reactive Carbonyl Species:  
491 A Comparative Study. *ChemMedChem*, 1778–1789.  
492 <https://doi.org/10.1002/cmdc.201500552>

493 Estévez, L., & Mosquera, R. A. (2009). Conformational and substitution effects on the  
494 electron distribution in a series of anthocyanidins. *Journal of Physical Chemistry A*,  
495 113(36), 9908–9919. <https://doi.org/10.1021/jp904298z>

496 Goufo, P., & Trindade, H. (2014). Rice antioxidants: phenolic acids, flavonoids,  
497 anthocyanins, proanthocyanidins, tocopherols, tocotrienols,  $\gamma$ -oryzanol, and phytic  
498 acid. *Food Science & Nutrition*, 2(2), 75–104. <https://doi.org/10.1002/fsn3.86>

499 Keller, B. O., Sui, J., Young, A. B., & Whittall, R. M. (2008). Interferences and contaminants  
500 encountered in modern mass spectrometry. *Analytica Chimica Acta*.  
501 <https://doi.org/10.1016/j.aca.2008.04.043>

502 Kim, J. Y., Seo, W. D., Park, D. S., Jang, K. C., Choi, K. J., Kim, S. Y., ... Han, S. I.  
503 (2013). Comparative studies on major nutritional components of black waxy rice with  
504 giant embryos and its rice bran. *Food Science and Biotechnology*, 22(SUPPL. 1),  
505 121–128. <https://doi.org/10.1007/s10068-013-0057-1>

506 Kiyooka, S. I., Kaneno, D., & Fujiyama, R. (2013). Parr's index to describe both  
507 electrophilicity and nucleophilicity. *Tetrahedron Letters*, 54(4), 339–342.  
508 <https://doi.org/10.1016/j.tetlet.2012.11.039>

509 Lee, Y.-M., Han, S.-I., Song, B. C., & Yeum, K.-J. (2015). Bioactives in Commonly

510 Consumed Cereal Grains: Implications for Oxidative Stress and Inflammation. *Journal*  
511 *of Medicinal Food*, 18(11), 1179–1186. <https://doi.org/10.1089/jmf.2014.3394>

512 Masisi, K., Beta, T., & Moghadasian, M. H. (2016). Antioxidant properties of diverse cereal  
513 grains: A review on in vitro and in vivo studies. *Food Chemistry*.  
514 <https://doi.org/10.1016/j.foodchem.2015.09.021>

515 Pereira-Caro, G., Cros, G., Yokota, T., & Crozier, A. (2013). Phytochemical profiles of  
516 black, red, brown, and white rice from the camargue region of France. *Journal of*  
517 *Agricultural and Food Chemistry*, 61(33), 7976–7986.  
518 <https://doi.org/10.1021/jf401937b>

519 Poli, G., & Schaur, R. J. (2000). 4-Hydroxynonenal in the pathomechanisms of oxidative  
520 stress. *IUBMB Life*. <https://doi.org/10.1080/15216540051081092>

521 Poli, G., Schaur, R. J., Siems, W. G., & Leonarduzzi, G. (2008). 4-hydroxynonenal: a  
522 membrane lipid oxidation product of medicinal interest. *Medicinal Research Reviews*,  
523 28(4), 569–631. <https://doi.org/10.1002/med.20117>

524 Rees, M. S., van Kuijk, F. J. G. M., Siakotos, A. N., & Mundy, B. P. (1995). Improved  
525 synthesis of various isotope labeled 4-hydroxyalkenals and peroxidation  
526 intermediates. *Synthetic Communications*, 25(20), 3225–3236.  
527 <https://doi.org/10.1080/00397919508015474>

528 Schaur, R. J., Siems, W., Bresgen, N., & Eckl, P. M. (2015). 4-hydroxy-nonenal—a  
529 bioactive lipid peroxidation product. *Biomolecules*, 5(4), 2247–2337.  
530 <https://doi.org/10.3390/biom5042247>

531 Schmidt, M. W., Baldrige, K. K., Boatz, J. A., Elbert, S. T., Gordon, M. S., Jensen, J. H.,  
532 ... Montgomery, J. A. (1993). General atomic and molecular electronic structure  
533 system. *Journal of Computational Chemistry*, 14(11), 1347–1363.  
534 <https://doi.org/10.1002/jcc.540141112>

535 Surh, J., & Kwon, H. (2005). Estimation of daily exposure to 4-hydroxy-2-alkenals in  
536 Korean foods containing n-3 and n-6 polyunsaturated fatty acids. *Food Additives and*  
537 *Contaminants*, 22(8), 701–708. <https://doi.org/10.1080/02652030500164359>

538 Suttiarporn, P., Chumpolsri, W., Mahatheeranont, S., Luangkamin, S., Teepsawang, S., &  
539 Leardkamolkarn, V. (2015). Structures of phytosterols and triterpenoids with potential  
540 anti-cancer activity in bran of black non-glutinous rice. *Nutrients*, 7(3), 1672–1687.  
541 <https://doi.org/10.3390/nu7031672>

542 Vistoli, G., Orioli, M., Pedretti, A., Regazzoni, L., Canevotti, R., Negrisoni, G., ... Aldini, G.  
543 (2009). Design, synthesis, and evaluation of carnosine derivatives as selective and



544 efficient sequestering agents of cytotoxic reactive carbonyl species. *ChemMedChem*,  
 545 4(6), 967–975. <https://doi.org/10.1002/cmdc.200800433>  
 546 Zhu, Q., Zheng, Z. P., Cheng, K. W., Wu, J. J., Zhang, S., Yun, S. T., ... Wang, M. (2009).  
 547 Natural polyphenols as direct trapping agents of lipid peroxidation-derived acrolein  
 548 and 4-hydroxy-trans-2-nonenal. *Chemical Research in Toxicology*, 22(10), 1721–  
 549 1727. <https://doi.org/10.1021/tx900221s>

550

## 551 **Tables**

552

553 **Table 1** - HNE sequestering activity of rice extracts. Activities are reported as IC<sub>50</sub> which  
 554 represents the concentration of the tested compound able to reduce by 50% HNE-induced  
 555 ubiquitin carbonylation.

556

Rice extract	Average IC <sub>50</sub> (mg/mL)	SD	CV%
Black rice giant embryo (BRGE)	29.10	0.79	2.7
Black rice giant embryo bran	30.63	3.70	12.4
Miryang282	39.32	2.48	6.3
White rice (brown)	45.46	2.29	5
Black rice	52.04	8.34	16
Black rice giant embryo 2 (BRGE2)	65.92	2.13	3.2
Red rice	71.32	4.04	5.7
White rice (brown)	151.00	17.70	11.7

557

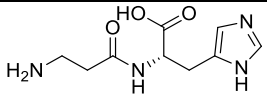
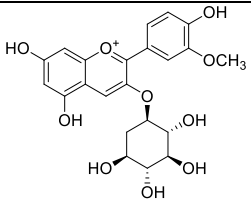
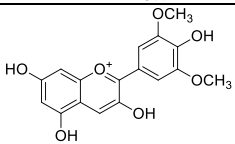
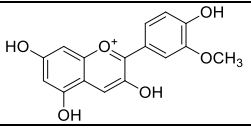
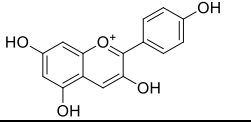
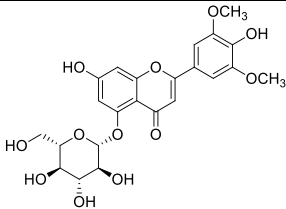
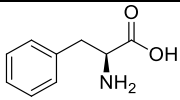
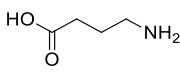
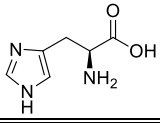
558 **Table 2** – HNE quenchers identified in rice extract BRGE by using the isotopic labelling  
 559 procedure.

560

Quencher monoisotopic MW	Calculated MW	Δppm	Possible structure
103.06336	103.06333	0.304	γ-Aminobutirric acid
155.06950	155.06948	0.151	Histidine
165.07922	165.07898	1.462	Phenylalanine
271.06133	271.06064	2.514	Pelargonidin
301.07236	301.07121	3.809	Peonidin
317.06864	317.06612	7.923	Petunidin
317.12164	317.12229	-2.082	Asp-Ser-Pro
330.07634	330.07395	7.232	Tricin
331.08361	331.08177	5.533	Malvidin

561

562 **Table 3** – HNE sequestering activity of standard compounds identified in rice extract  
 563 BRGE. Activity was determined by measuring free-HNE by HPLC-UV analysis.  
 564

		ACTIVITY (CARNOSINE UNITS)		HNE CONSUMPTION (%)	
		1h	3h	1h	3h
<b>REFERENCE COMPOUNDS</b>					
<i>Buffer</i>		< 0.10	< 0.10	0.17±0.31	0.71±0.67
<i>Carnosine</i>		1.00	1.00	13.78±2.34	36.06±4.98
<b>POLYPHENOLS</b>					
<i>Peonidin-3-O-glucoside</i>		0.29	0.20	4.00±1.39	7.27±2.42
<i>Malvidin</i>		< 0.10	< 0.10	1.15±1.10	1.87±1.35
<i>Peonidin</i>		< 0.10	0.12	1.02±0.47	4.31±0.92
<i>Pelargonidin</i>		0.57	0.35	7.81±0.49	12.60±1.99
<i>Tricin-5-O-glucoside</i>		0.30	0.20	5.03±2.58	8.31±2.91
<b>AMINOACIDS</b>					
<i>Phenylalanine</i>		< 0.10	< 0.10	0.84±0.78	1.28±0.47
<i>GABA</i>		< 0.10	< 0.10	0.34±0.59	0.35±0.62
<i>Histidine</i>		0.12	0.17	1.77±1.82	6.26±2.69

565  
 566 **Table 4** - DFT-based properties of the three major tautomer of malvidin and pelargonidin  
 567 ( $\Delta E$  values are expressed in kJ/mol; nucleophilicity descriptors are based on the Parr's  
 568 indices as  $Nucleo = 1/\omega$  (Kiyooka, Kaneno, & Fujiyama, 2013)).

569

<b>Compound</b>	<b>Nucleo_N5</b>	<b>Nucleo_N7</b>	<b>Nucleo_N4'</b>	<b><math>\Delta E_{N5}</math></b>	<b><math>\Delta E_{N7}</math></b>	<b><math>\Delta E_{N4'}</math></b>
<i>Malvidin</i>	5.18	5.08	4.86	0.00	+9.59	+15.63
<i>Pelargonidin</i>	5.15	5.29	4.60	+7.78	0.00	+18.27

570

571